

# The effect of spin-orbit coupling on the effective-spin correlation in YbMgGaO<sub>4</sub>

Yao-Dong Li<sup>1</sup>, Yao Shen<sup>1</sup>, Yuesheng Li<sup>2,3</sup>, Jun Zhao<sup>1,4</sup>, and Gang Chen<sup>1,4\*</sup>

<sup>1</sup>State Key Laboratory of Surface Physics, Center for Field Theory and Particle Physics, Department of Physics, Fudan University, Shanghai 200433, People's Republic of China

<sup>2</sup>Department of Physics, Renmin University of China, Beijing 100872, People's Republic of China

<sup>3</sup>Experimental Physics VI, Center for Electronic Correlations and Magnetism, University of Augsburg, 86159 Augsburg, Germany and

<sup>4</sup>Collaborative Innovation Center of Advanced Microstructures, Nanjing, 210093, People's Republic of China

(Dated: September 13, 2016)

Motivated by the recent experiments on the triangular lattice spin liquid YbMgGaO<sub>4</sub>, we explore the effect of spin-orbit coupling on the effective-spin correlation of the Yb local moments. We point out the anisotropic interaction between the effective-spins on the nearest neighbor bonds is sufficient to reproduce the spin-wave dispersion of the fully polarized state in the presence of strong magnetic field normal to the triangular plane. We further evaluate the effective-spin correlation within the mean-field spherical approximation. We explicitly demonstrate that, the nearest-neighbor anisotropic effective-spin interaction, originating from the strong spin-orbit coupling, enhances the effective-spin correlation at the M points in the Brillouin zone. We identify these results as the strong evidence for the anisotropic interaction and the strong spin-orbit coupling in YbMgGaO<sub>4</sub>.

## I. INTRODUCTION

The rare earth triangular lattice antiferromagnet YbMgGaO<sub>4</sub> was recently proposed to be a candidate for quantum spin liquid (QSL)<sup>1–5</sup>. In YbMgGaO<sub>4</sub>, the Yb<sup>3+</sup> ions form a perfect two-dimensional triangular lattice. For the Yb<sup>3+</sup> ions, the strong spin-orbit coupling (SOC) entangles the orbital angular momentum,  $\mathbf{L}$  ( $L = 3$ ), with the total spin,  $\mathbf{s}$  ( $s = 1/2$ ), leading to a total moment,  $\mathbf{J}$  ( $J = 7/2$ )<sup>1,2</sup>. Like the case in the spin ice material Yb<sub>2</sub>Ti<sub>2</sub>O<sub>7</sub><sup>6</sup>, the crystal electric field in YbMgGaO<sub>4</sub> further splits the eight-fold degeneracy of the Yb<sup>3+</sup> total moment into four Kramers' doublets. The ground state Kramers' doublet is separated from the excited doublets by a crystal field energy gap. At the temperature that is much lower than the crystal field gap, the magnetic properties of YbMgGaO<sub>4</sub> are fully described by the ground state Kramers' doublets<sup>2</sup>. The ground state Kramers' doublet is modeled by an effective-spin-1/2 local moment  $\mathbf{S}$ . Therefore, YbMgGaO<sub>4</sub> is regarded as a QSL with effective-spin-1/2 local moments on a triangular lattice<sup>1–4</sup>.

The existing experiments on YbMgGaO<sub>4</sub> have involved thermodynamic, neutron scattering, and  $\mu$ SR measurements<sup>1,3–5</sup>. The system was found to remain disordered down to 0.05K in the recent  $\mu$ SR measurement<sup>5</sup>. The thermodynamic measurement finds a constant magnetic susceptibility in the zero temperature limit. In the low temperature regime, the heat capacity<sup>1,4</sup> behaves as  $C_v \approx \text{constant} \times T^{0.7}$ . The inelastic neutron scattering measurements from two research groups have found the presence of broad magnetic excitation continuum<sup>3,4</sup>. In particular, the inelastic neutron scattering results from Yao Shen *et al* clearly indicate the upper excitation edge and the *dispersive* continuum of magnetic excitations<sup>3</sup>. Both neutron scattering results found a weak spectral peak at the M points in the Brillouin zone<sup>3,4</sup>. Based on the existing experiments, we have proposed that the

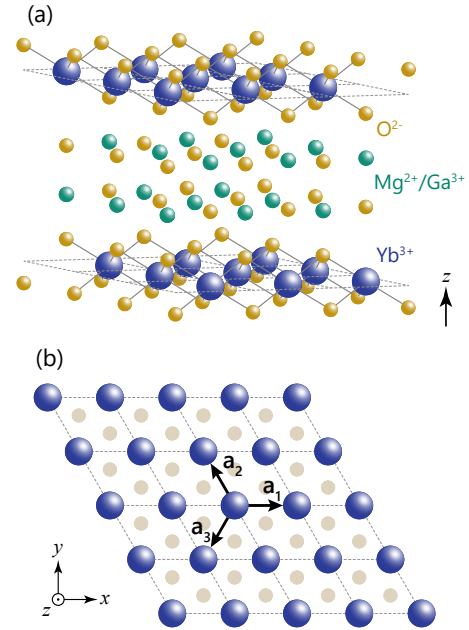


FIG. 1. (Color online.) (a) The crystal structure of YbMgGaO<sub>4</sub>. Mg and Ga ions form the non-magnetic layer. (b) The Yb triangular layer.

spinon Fermi surface U(1) QSL gives a reasonable description of the experimental results<sup>3</sup>.

Previously, two organic triangular antiferromagnets,  $\kappa$ -(ET)<sub>2</sub>Cu<sub>2</sub>(CN)<sub>3</sub> and EtMe<sub>3</sub>Sb[Pd(dmit)<sub>2</sub>]<sub>2</sub>, were proposed to be QSLs<sup>7–10</sup>. These two materials are in the weak Mott regime, where the charge fluctuation is strong. It was then suggested that the four-spin ring exchange interaction due to the strong charge fluctuation may destabilize the magnetic order and favor a QSL ground state<sup>11,12</sup>. Unlike the organic counterparts, YbMgGaO<sub>4</sub> is in the strong Mott regime<sup>1,2</sup>. The 4f electrons of the

$\text{Yb}^{3+}$  ion is very localized spatially. As a result, the physical mechanism for the QSL ground state in this new material is deemed to be quite different. The new ingredient of the new material is the strong SOC and the spin-orbit entangled nature of the  $\text{Yb}^{3+}$  local moment. It was pointed out that the spin-orbit entanglement leads to highly anisotropic interactions between the Yb local moments<sup>2,13–15</sup>. The anisotropic effective-spin interaction is shown to enhance the quantum fluctuation and suppress the magnetic order in a large parameter regime where the QSL may be located<sup>2</sup>. On the fundamental side, it was recently argued that, as long as the time reversal symmetry is preserved, the ground state of a spin-orbit-coupled Mott insulator with odd number of electrons per cell must be exotic<sup>16</sup>. This theoretical argument implies that the spin-orbit-coupled Mott insulator can in principle be candidates for spin liquids.  $\text{YbMgGaO}_4$  falls into this class and is actually the first such material.

More recently, Ref. 4 introduced the XXZ exchange interactions on both nearest-neighbor and next-nearest-neighbor sites to account for the spin-wave dispersion in the strong magnetic field and the weak peak at the M points in the effective-spin correlations. The authors further suggested the further neighbor competing exchange interactions as the possible mechanism for the QSL in  $\text{YbMgGaO}_4$ . In this paper, however, we focus on the anisotropic effective-spin interactions on the nearest-neighbor sites. After carefully justifying the underlying microscopics that supports the nearest-neighbor anisotropic model, we demonstrate that the nearest-neighbor model is sufficient to reproduce the spin-wave dispersion of the polarized state in the strong magnetic field. With the nearest-neighbor anisotropic model, we further show that the effective-spin correlation also develops a peak at the M points. Therefore, we think the nearest-neighbor anisotropic model captures the essential physics for  $\text{YbMgGaO}_4$ .

The remaining part of the paper is outlined as follows. In Sec. II, we describe some of the details about the microscopics of the interactions between the Yb local moments. In Sec. III, we compare the spin-wave dispersion of the nearest-neighbor anisotropic interactions in a strong field with the existing experimental data. In Sec. IV, we evaluate the effective-spin correlation from the effective-spin models with and without the anisotropic interaction. Finally in Sec. V, we conclude with a discussion.

## II. THE ANISOTROPIC INTERACTION FOR THE EFFECTIVE SPINS

Compared to the organic spin liquid candidates<sup>7–10</sup>,  $\text{YbMgGaO}_4$  is in the strong Mott regime, and the charge fluctuation is rather weak. Therefore, the four-spin ring exchange, that is a higher order perturbative process than the nearest-neighbor pairwise interaction, is strongly suppressed. In the previous work<sup>1,2</sup>,

we have proposed that the generic pairwise effective-spin interaction for the nearest-neighbor Yb moments in  $\text{YbMgGaO}_4$ ,

$$\begin{aligned} \mathcal{H} = & \sum_{\langle \mathbf{r}\mathbf{r}' \rangle} J_{zz} S_{\mathbf{r}}^z S_{\mathbf{r}'}^z + J_{\pm} (S_{\mathbf{r}}^+ S_{\mathbf{r}'}^- + S_{\mathbf{r}}^- S_{\mathbf{r}'}^+) \\ & + J_{\pm\pm} (\gamma_{\mathbf{r}\mathbf{r}'} S_{\mathbf{r}}^+ S_{\mathbf{r}'}^+ + \gamma_{\mathbf{r}\mathbf{r}'}^* S_{\mathbf{r}}^- S_{\mathbf{r}'}^-) \\ & - \frac{iJ_{z\pm}}{2} [(\gamma_{\mathbf{r}\mathbf{r}'}^* S_{\mathbf{r}}^+ - \gamma_{\mathbf{r}\mathbf{r}'} S_{\mathbf{r}}^-) S_{\mathbf{r}'}^z \\ & + S_{\mathbf{r}}^z (\gamma_{\mathbf{r}\mathbf{r}'}^* S_{\mathbf{r}'}^+ - \gamma_{\mathbf{r}\mathbf{r}'} S_{\mathbf{r}'}^-)], \end{aligned} \quad (1)$$

where  $S_{\mathbf{r}}^{\pm} = S_{\mathbf{r}}^x \pm iS_{\mathbf{r}}^y$ , and  $\gamma_{\mathbf{r}\mathbf{r}'} = \gamma_{\mathbf{r}'\mathbf{r}} = 1, e^{i2\pi/3}, e^{-i2\pi/3}$  are the phase factors for the bond  $\mathbf{r}\mathbf{r}'$  along the  $\mathbf{a}_1, \mathbf{a}_2, \mathbf{a}_3$  directions (see Fig. 1). The  $J_{\pm\pm}$  and  $J_{z\pm}$  terms of Eq. (1) are anisotropic interactions arising naturally from the strong SOC. Due to the SOC, the effective-spins inherit the symmetry operation of the space group, hence there are bond-dependent  $J_{\pm\pm}$  and  $J_{z\pm}$  interactions.

Our generic model in Eq. (1) contains the contribution from all microscopic processes that include the direct  $4f$ -electron exchange, the indirect exchange through the intermediate oxygen ions, and the dipole-dipole interaction. The further neighbor interaction is neglected in our generic model. Like the ring exchange, the further neighbor superexchange usually involves higher order perturbative processes via multiple steps of electron tunnelings than the nearest-neighbor interactions. Even though the further neighbor superexchange interaction can be mediated by the direct electron hoppings between these sites, the contribution should be very small due to the very localized nature of the  $4f$  electron wavefunction. The remaining contribution is the further neighbor dipole-dipole interaction. For the next-nearest neighbors, the dipole-dipole interaction is estimated to be  $\sim 0.01$ – $0.02\text{K}$  and is thus one or two orders of magnitude smaller than the nearest-neighbor interactions. Therefore, we can safely neglect the further neighbor interactions and only keep the nearest neighbor ones in Eq. (1).

The large chemical difference prohibits the Ga or Mg contamination in the Yb layers. The Yb layers are kept clean, and there is little disorder in the exchange interaction. Although there exists Ga/Mg mixing in the nonmagnetic layers, the exchange path that they involve would be Yb-O-Ga-O-Yb or Yb-O-Mg-O-Yb (see Fig. 1). This exchange path is a higher order perturbative process than the Yb-O-Yb one and thus can be neglected. We do not expect the Ga/Mg mixing in the nonmagnetic layers to cause much exchange disorder within the Yb layers. The Ga/Mg disorder in  $\text{YbMgGaO}_4$  is different from the Cu/Zn disorder in herbertsmithite<sup>17–20</sup>. In the latter case, the Cu disorder carries magnetic moment and directly couples to the spin in the Cu layers.

The XXZ limit of our generic model has already been studied in some of the early works<sup>21,22</sup>. It was shown that the magnetic ordered ground state was obtained for all parameter regions in the XXZ limit. To obtain a disordered ground state for the generic model, it is necessary to have the  $J_{\pm\pm}$  and  $J_{z\pm}$  interactions. In Ref. 2, we have

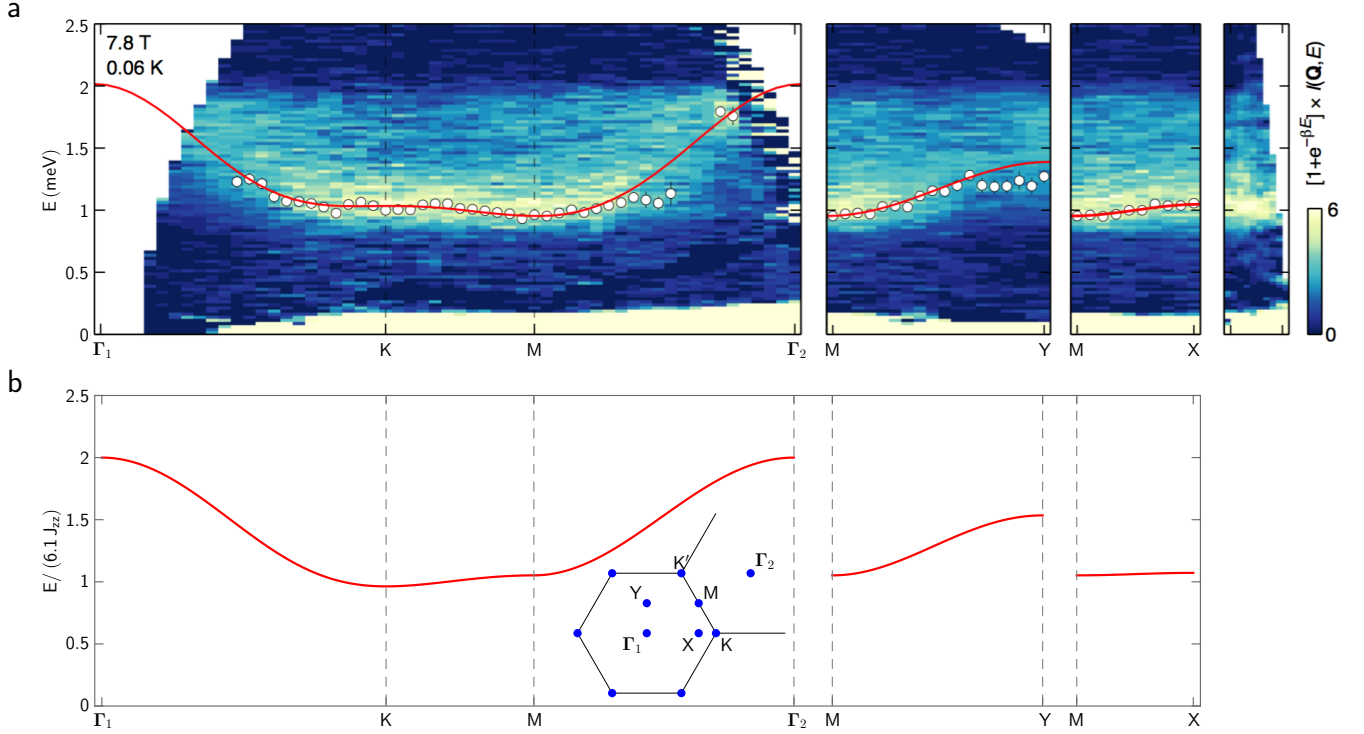


FIG. 2. (Color online.) (a) The experimental spin-wave dispersion in the presence of external field along  $z$ -direction with field strength 7.8T at 0.06K (adapted from Ref. 4). According to Ref. 4, the white circles indicate the location of the maximum intensity. The error bar, however, was not indicated in the plot. The red lines show a fit to the spin-wave dispersion relation that is obtained after including both nearest-neighbor and next-nearest-neighbor XXZ exchange interactions<sup>4</sup>. (b) The theoretical spin-wave dispersion according to the nearest-neighbor anisotropic exchange model Eq. (1), where we set  $J_{\pm}/J_{zz} = 0.66$ ,  $J_{\pm\pm}/J_{zz} = 0.34$ , and  $\hbar/J_{zz} = 10.5$ . The analytical expression of the dispersion is given in Eq. (2). The inset of (b) is the Brillouin zone.

shown that the 120-degree magnetic order in the XXZ limit is actually destabilized by the enhanced quantum fluctuation when the anisotropic  $J_{\pm\pm}$  and  $J_{z\pm}$  interactions are introduced.

### III. SPIN-WAVE DISPERSION IN THE STRONG MAGNETIC FIELD

The nearest-neighbor interaction between the Yb local moments are of the order of several Kelvins<sup>1</sup>; as a result, a moderate magnetic field in the lab is sufficient for polarizing the local moment<sup>2</sup>. Under the linear spin-wave approximation, the spin-wave dispersion in the presence of the strong external magnetic field is given as<sup>2</sup>

$$\omega_z(\mathbf{k}) = \left\{ [g_z \mu_B B_z - 3J_{zz} + 2J_{\pm} \sum_{i=1}^3 \cos(\mathbf{k} \cdot \mathbf{a}_i)]^2 - 4J_{\pm\pm}^2 [\cos(\mathbf{k} \cdot \mathbf{a}_1) + e^{-i\frac{2\pi}{3}} \cos(\mathbf{k} \cdot \mathbf{a}_2) + e^{i\frac{2\pi}{3}} \cos(\mathbf{k} \cdot \mathbf{a}_3)]^2 \right\}^{1/2}, \quad (2)$$

where  $g_z$  and  $B_z$  are Landé factor and magnetic field along  $z$ -direction, respectively. Notice that the dispersion

in Eq. (2) is independent of  $J_{z\pm}$ ; this is an artifact of the linear spin-wave approximation.

In the recent experiment in Ref. 4, a magnetic field of 7.8T normal to the Yb plane at 0.06K, a gapped magnon band structure is observed. In Fig. 2, we compare our theoretical result with a tentative choice of exchange couplings in Eq. (2) with the experimental results from Ref. 4. Since the error bar is not known from Ref. 4, judging from the extension of the bright region in Fig. 2a, we would think that the agreement between the theoretical result and the experimental result is reasonable. Here, we have to mention that the dispersion that is plotted in Fig. 2 is not quite sensitive to the choice of  $J_{\pm\pm}$ . Therefore, we expect it is better to combine the spin-wave dispersion for several field orientations and to extract the exchange couplings more accurately. For an arbitrary external field in the  $xz$  plane, the Hamiltonian is given by

$$\mathcal{H}_{xz} = \mathcal{H} - \sum_{\mathbf{r}} \mu_B [g_x B_x S_{\mathbf{r}}^x + g_z B_z S_{\mathbf{r}}^z]. \quad (3)$$

Since  $g_x \neq g_z$ , the uniform magnetization,  $\mathbf{m} \equiv \langle \mathbf{S}_{\mathbf{r}} \rangle$ , is generally not parallel to the external magnetic field. For  $B_x \equiv B \sin \theta$  and  $B_z \equiv B \cos \theta$ , the magnetization is

given by

$$\mathbf{m} = m(\hat{x} \sin \theta' + \hat{z} \cos \theta'), \quad (4)$$

where  $\tan \theta' = (g_x/g_z) \tan \theta$ . At a sufficiently large magnetic field, all the moments are polarized along the direction defined by  $\theta'$ . In the linear spin-wave theory for this polarized state, we choose the magnetization to be the quantization axis for the Holstein-Primakoff transforma-

tion,

$$\mathbf{S}_\mathbf{r} \cdot \frac{\mathbf{m}}{|\mathbf{m}|} \equiv \frac{1}{2} - a_\mathbf{r}^\dagger a_\mathbf{r}, \quad (5)$$

$$\mathbf{S}_\mathbf{r} \cdot \hat{y} \equiv \frac{1}{2}(a_\mathbf{r} + a_\mathbf{r}^\dagger), \quad (6)$$

$$\mathbf{S}_\mathbf{r} \cdot \left(\frac{\mathbf{m}}{|\mathbf{m}|} \times \hat{y}\right) \equiv \frac{1}{2i}(a_\mathbf{r} - a_\mathbf{r}^\dagger), \quad (7)$$

where  $a_\mathbf{r}^\dagger$  ( $a_\mathbf{r}$ ) is the creation (annihilation) operator for the Holstein-Primakoff boson. In the linear spin-wave approximation, we plug the Holstein-Primakoff transformation into  $\mathcal{H}_{xz}$  and keep the quadratic part of the the Holstein-Primakoff bosons. The spin-wave dispersion is obtained by solving the linear spin-wave Hamiltonian and is given by

$$\begin{aligned} \omega_{xz}(\mathbf{k}) = & \left\{ \left[ g_x \mu_B B_x \sin \theta' + g_z \mu_B B_z \cos \theta' - 6J_\pm \sin^2 \theta' - 3J_{zz} \cos^2 \theta' + \cos(\mathbf{k} \cdot \mathbf{a}_1) \left( \frac{J_\pm}{2} (3 + \cos 2\theta') \right. \right. \right. \\ & - J_{\pm\pm} \sin^2 \theta' + \frac{J_{zz}}{2} \sin^2 \theta' \Big) + \cos(\mathbf{k} \cdot \mathbf{a}_2) \left( \frac{J_\pm}{2} (3 + \cos 2\theta') + \frac{J_{\pm\pm}}{2} \sin^2 \theta' + \frac{J_{zz}}{2} \sin^2 \theta' \right. \\ & + \frac{\sqrt{3}}{4} J_{z\pm} \sin 2\theta' \Big) + \cos(\mathbf{k} \cdot \mathbf{a}_3) \left( \frac{J_\pm}{2} (3 + \cos 2\theta') + \frac{J_{\pm\pm}}{2} \sin^2 \theta' + \frac{J_{zz}}{2} \sin^2 \theta' - \frac{\sqrt{3}}{4} J_{z\pm} \sin 2\theta' \right) \Big]^2 \\ & - \left| \cos(\mathbf{k} \cdot \mathbf{a}_1) \left( J_\pm \sin^2 \theta' - J_{\pm\pm} (1 + \cos^2 \theta') - iJ_{z\pm} \sin \theta' - \frac{J_{zz}}{2} \sin^2 \theta' \right) \right. \\ & + \cos(\mathbf{k} \cdot \mathbf{a}_2) \left( J_\pm \sin^2 \theta' + \frac{J_{\pm\pm}}{4} (3 + \cos 2\theta' - 4i\sqrt{3} \cos \theta') - \frac{J_{zz}}{2} \sin^2 \theta' + \frac{J_{z\pm}}{4} (2i \sin \theta' - \sqrt{3} \sin 2\theta') \right) \\ & \left. \left. + \cos(\mathbf{k} \cdot \mathbf{a}_3) \left( J_\pm \sin^2 \theta' + \frac{J_{\pm\pm}}{4} (3 + \cos 2\theta' + 4i\sqrt{3} \cos \theta') - \frac{J_{zz}}{2} \sin^2 \theta' + \frac{J_{z\pm}}{4} (2i \sin \theta' + \sqrt{3} \sin 2\theta') \right) \right| \right\}^{1/2}. \quad (8) \end{aligned}$$

Likewise, for the field within the  $xy$  plane, the Hamiltonian is given by

$$\mathcal{H}_{xy} = \mathcal{H} - \sum_{\mathbf{r}} \mu_B [g_x B_x S_\mathbf{r}^x + g_y B_y S_\mathbf{r}^y]. \quad (9)$$

Now because of the three-fold on-site symmetry,  $g_x = g_y$ . The magnetization is parallel to the external magnetic field. For  $B_x \equiv B \cos \phi$  and  $B_y \equiv B \sin \phi$ , the magnetization is  $\mathbf{m} = m(\hat{x} \cos \phi + \hat{y} \sin \phi)$ , and the corresponding spin-wave dispersion in the strong field limit is given by

$$\begin{aligned} \omega_{xy}(\mathbf{k}) = & \left\{ \left[ g_x \mu_B B_x \cos \phi + g_y \mu_B B_y \sin \phi - 6J_\pm + \cos(\mathbf{k} \cdot \mathbf{a}_1) \left( J_\pm + \frac{J_{zz}}{2} - J_{\pm\pm} \cos 2\phi \right) \right. \right. \\ & + \cos(\mathbf{k} \cdot \mathbf{a}_2) \left( J_\pm + \frac{J_{zz}}{2} + J_{\pm\pm} \cos(2\phi - \frac{\pi}{3}) \right) + \cos(\mathbf{k} \cdot \mathbf{a}_3) \left( J_\pm + \frac{J_{zz}}{2} + J_{\pm\pm} \cos(2\phi + \frac{\pi}{3}) \right) \Big]^2 \\ & - \left| \cos(\mathbf{k} \cdot \mathbf{a}_1) \left( J_\pm - \frac{J_{zz}}{2} - J_{\pm\pm} \cos 2\phi + iJ_{z\pm} \cos \phi \right) + \cos(\mathbf{k} \cdot \mathbf{a}_2) \left( J_\pm - \frac{J_{zz}}{2} + J_{\pm\pm} \cos(2\phi + \frac{\pi}{3}) \right. \right. \\ & \left. \left. - iJ_{z\pm} \cos(\phi - \frac{\pi}{3}) \right) + \cos(\mathbf{k} \cdot \mathbf{a}_3) \left( J_\pm - \frac{J_{zz}}{2} + J_{\pm\pm} \cos(2\phi - \frac{\pi}{3}) - iJ_{z\pm} \cos(\phi + \frac{\pi}{3}) \right) \right| \right\}^{1/2}. \quad (10) \end{aligned}$$

#### IV. EFFECTIVE-SPIN CORRELATION

In both Ref. 3 and Ref. 4, a weak spectral peak at the M points is found in the inelastic neutron scattering data. This result indicates that the interaction between the Yb local moments enhances the correlation of the effective-spins at the M points. Actually in Ref. 2, we have already

shown that, the anisotropic  $J_{\pm\pm}$  and  $J_{z\pm}$  interactions, if they are significant, would favor a stripe magnetic order with an ordering wavevector at the M points<sup>23</sup>. This theoretical result immediately means that the anisotropic  $J_{\pm\pm}$  and  $J_{z\pm}$  interactions would enhance the effective-spin correlation at the M points. In the following, we demonstrate explicitly that the generic model in Eq. (1)

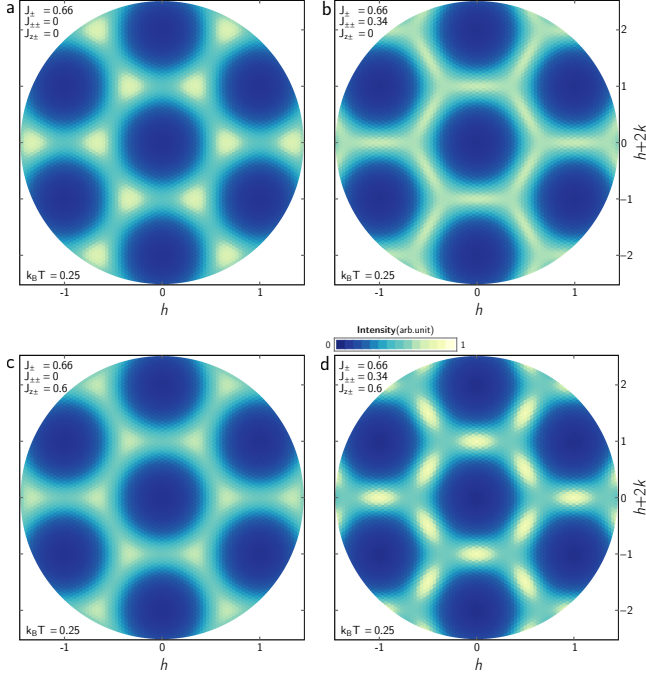


FIG. 3. (Color online.) Contour plot of effective-spin correlation  $\langle S_{\mathbf{k}}^+ S_{-\mathbf{k}}^- \rangle$  in the momentum space. The correlation function is computed from the nearest-neighbor model in Eq. (1), with parameters in units of  $J_{zz}$  indicated. Without the anisotropic exchanges, the spectral weight peaks around K. The anisotropic  $J_{\pm\pm}$  and  $J_{z\pm}$  interactions can switch the peak to M.

with the anisotropic nearest-neighbor interactions does enhance the effective-spin correlation at the M points. We start from the mean-field partition function of the system,

$$\begin{aligned} \mathcal{Z} &= \int \mathcal{D}[\mathbf{S}_{\mathbf{r}}] \prod_{\mathbf{r}} \delta(\mathbf{S}_{\mathbf{r}}^2 - S^2) e^{-\beta \mathcal{H}} \\ &= \int \mathcal{D}[\mathbf{S}_{\mathbf{r}}] \mathcal{D}[\lambda_{\mathbf{r}}] e^{-\beta \mathcal{H} + \sum_{\mathbf{r}} \lambda_{\mathbf{r}} [\mathbf{S}_{\mathbf{r}}^2 - S^2]} \\ &\equiv \int \mathcal{D}[\mathbf{S}_{\mathbf{r}}] \mathcal{D}[\lambda_{\mathbf{r}}] e^{-\mathcal{S}_{\text{eff}}[\beta, \lambda_{\mathbf{r}}]}, \end{aligned} \quad (11)$$

where  $\mathcal{H}$  is given in Eq. (1),  $\mathcal{S}_{\text{eff}}$  is the effective action that describes the effective-spin interaction, and  $\lambda_{\mathbf{r}}$  is the local Lagrange multiplier that imposes the local constraint with  $|\mathbf{S}_{\mathbf{r}}|^2 = S^2$ . Although this mean-field approximation does not give the quantum ground state, it does provide a qualitative understanding about the relationship between the effective-spin correlation and the microscopic spin interactions.

To evaluate the effective-spin correlation, we here adopt a spherical approximation<sup>24</sup> by replacing the local constraint with a global one such that  $\sum_{\mathbf{r}} |\mathbf{S}_{\mathbf{r}}|^2 = N_{\text{site}} S^2$ , where  $N_{\text{site}}$  is the total number of lattice sites. This approximation is equivalent to choosing a uniform Lagrange multiplier with  $\lambda_{\mathbf{r}} \equiv \lambda$ . It has been shown that

the spin correlations determined from classical Monte Carlo simulation are described quantitatively within this scheme<sup>24</sup>.

In the momentum space, we define

$$S_{\mathbf{r}}^{\mu} \equiv \frac{1}{\sqrt{N_{\text{site}}}} \sum_{\mathbf{k} \in \text{BZ}} S_{\mathbf{k}}^{\mu} e^{i\mathbf{k} \cdot \mathbf{r}}, \quad (12)$$

and the effective action is given by

$$\begin{aligned} \mathcal{S}_{\text{eff}}[\beta, \lambda] &= \sum_{\mathbf{k} \in \text{BZ}} \beta [\mathcal{J}_{\mu\nu}(\mathbf{k}) + \Delta(\beta) \delta_{\mu\nu}] S_{\mathbf{k}}^{\mu} S_{-\mathbf{k}}^{\nu} \\ &\quad - \beta N_{\text{site}} \Delta(\beta) S^2, \end{aligned} \quad (13)$$

where we have placed  $\lambda \equiv -\beta \Delta(\beta)$  in a saddle point approximation,  $\mu, \nu = x, y, z$ , and  $\mathcal{J}_{\mu\nu}(\mathbf{k})$  is a  $3 \times 3$  exchange matrix that is obtained from Fourier transforming the exchange couplings. Note the XXZ part of the spin interactions only appears in the diagonal part of  $\mathcal{J}_{\mu\nu}(\mathbf{k})$  while the anisotropic  $J_{\pm\pm}$  and  $J_{z\pm}$  interactions are also present in the off-diagonal part. Hence the effective-spin correlation is given as

$$\langle S_{\mathbf{k}}^{\mu} S_{-\mathbf{k}}^{\nu} \rangle = \frac{1}{\beta} [\mathcal{J}(\mathbf{k}) + \Delta(\beta) \mathbb{1}_{3 \times 3}]_{\mu\nu}^{-1}, \quad (14)$$

where  $\mathbb{1}_{3 \times 3}$  is a  $3 \times 3$  identity matrix.

The saddle point equation is obtained by integrating out the effective-spins in the partition function and is given by

$$\sum_{\mathbf{k} \in \text{BZ}} \sum_{\mu} \frac{1}{\beta} [\mathcal{J}(\mathbf{k}) + \Delta(\beta) \mathbb{1}_{3 \times 3}]_{\mu\mu}^{-1} = N_{\text{site}} S^2, \quad (15)$$

from which, we determine  $\Delta(\beta)$  and the effective-spin correlation in Eq. (14).

The results of the effective-spin correlations are presented in Fig. 3. In the absence of the  $J_{\pm\pm}$  and  $J_{z\pm}$  interactions, the correlation function is peaked at the K points. This result is understood since the XXZ model favors the 120-degree state would simply enhance the effective-spin correlation at the K points that correspond to the ordering wavevectors of the 120-degree state. After we include the  $J_{\pm\pm}$  and  $J_{z\pm}$  interactions, the peak of the correlation function is switched to the M points (see Fig. 3d). This suggests that it is sufficient to have the  $J_{\pm\pm}$  and  $J_{z\pm}$  interactions in the nearest-neighbor model to account for the peak at the M points in the neutron scattering results.

## V. DISCUSSION

Instead of invoking further neighbor interaction in Ref. 4, we have focused on the anisotropic spin interaction on the nearest-neighbor bonds to account for the spin-wave dispersion of the polarized state in the strong magnetic field and the effective-spin correlation in YbMgGaO<sub>4</sub>. The bond-dependent interaction is a

natural and primary consequence of the strong SOC in the system. As for the importance of further neighbor interaction, it might be possible that some physical mechanism, that we are not aware of, may suppress the anisotropic spin interactions between the nearest neighbors but enhance the further neighbor spin interactions.

We have recently proposed that the spinon Fermi surface U(1) QSL provides a consistent explanation for the experimental results in YbMgGaO<sub>4</sub>. We pointed out that the particle-hole excitation of a simple non-interacting spinon Fermi sea already gives both the broad continuum and the upper excitation edge in the inelastic neutron scattering spectrum. In the future work, we will variationally optimize the energy against the trial ground state wavefunction that is constructed from a more generic spinon Fermi surface mean-field state. It will be ideal to directly compute the correlation function of the local

moments with respect to the variational ground state.

To summarize, we have provided a strong evidence of the anisotropic spin interaction and strong SOC in YbMgGaO<sub>4</sub>. In particular, the nearest-neighbor spin model, as used throughout the paper, proves to be the appropriate description of the system.

*Acknowledgements.*—G.C. sincerely acknowledges Dr. Martin Mourigal for discussion and appologizes for not informing him properly about adapting Fig. 2a. We thank Dr. Zhong Wang at IAS of Tsinghua University and Dr. Nanlin Wang at ICQM of Peking University for the hospitality during our visit in August 2016. This work is supported by the Start-up Funds of Fudan University (Shanghai, People's Republic of China) and the Thousand-Youth-Talent Program (G.C.) of People's Republic of China.

---

\* gangchen.physics@gmail.com,  
gchen.physics@fudan.edu.cn

- <sup>1</sup> Yuesheng Li, Gang Chen, Wei Tong, Li Pi, Juanjuan Liu, Zhaorong Yang, Xiaoqun Wang, and Qingming Zhang, "Rare-Earth Triangular Lattice Spin Liquid: A Single-Crystal Study of YbMgGaO<sub>4</sub>," *Phys. Rev. Lett.* **115**, 167203 (2015).
- <sup>2</sup> Yao-Dong Li, Xiaoqun Wang, and Gang Chen, "Anisotropic spin model of strong spin-orbit-coupled triangular antiferromagnets," *Phys. Rev. B* **94**, 035107 (2016).
- <sup>3</sup> Yao Shen, Yao-Dong Li, Hongliang Wo, Yuesheng Li, Shoudong Shen, Bingying Pan, Qisi Wang, H. C. Walker, P. Steffens, M Boehm, Yiqing Hao, D. L. Quintero-Castro, L. W. Harriger, Lijie Hao, Siqin Meng, Qingming Zhang, Gang Chen, and Jun Zhao, "Spinon fermi surface in a triangular lattice quantum spin liquid YbMgGaO<sub>4</sub>," arXiv preprint 1607.02615 (2016).
- <sup>4</sup> Joseph A. M. Paddison, Zhiling Dun, Georg Ehlers, Yao-hua Liu, Matthew B. Stone, Haidong Zhou, and Martin Mourigal, "Continuous excitations of the triangular-lattice quantum spin liquid YbMgGaO<sub>4</sub>," arXiv preprint 1607.03231 (2016).
- <sup>5</sup> Yuesheng Li, Devashibhai Adroja, Pabitra K. Biswas, Peter J. Baker, Qian Zhang, Juanjuan Liu, Alexander A. Tsirlin, Philipp Gegenwart, and Qingming Zhang, "μSR evidence for the U(1) quantum spin liquid ground state in the triangular antiferromagnet YbMgGaO<sub>4</sub>," arXiv preprint 1607.03298 (2016).
- <sup>6</sup> Kate A. Ross, Lucile Savary, Bruce D. Gaulin, and Leon Balents, "Quantum Excitations in Quantum Spin Ice," *Phys. Rev. X* **1**, 021002 (2011).
- <sup>7</sup> Y. Shimizu, K. Miyagawa, K. Kanoda, M. Maesato, and G. Saito, "Spin Liquid State in an Organic Mott Insulator with a Triangular Lattice," *Phys. Rev. Lett.* **91**, 107001 (2003).
- <sup>8</sup> T Itou, A Oyamada, S Maegawa, M Tamura, and R Kato, "Spin-liquid state in an organic spin-1/2 system on a triangular lattice, EtMe<sub>3</sub>Sb[Pd(dmit)<sub>2</sub>]<sub>2</sub>," *Journal of Physics: Condensed Matter* **19**, 145247 (2007).
- <sup>9</sup> Y. Kurosaki, Y. Shimizu, K. Miyagawa, K. Kanoda, and G. Saito, "Mott Transition from a Spin Liquid to a

- Fermi Liquid in the Spin-Frustrated Organic Conductor  $\kappa$ -(ET)<sub>2</sub>Cu<sub>2</sub>(CN)<sub>3</sub>," *Phys. Rev. Lett.* **95**, 177001 (2005).
- <sup>10</sup> T. Itou, A. Oyamada, S. Maegawa, M. Tamura, and R. Kato, "Quantum spin liquid in the spin-12 triangular antiferromagnet EtMe<sub>3</sub>Sb[Pd(dmit)<sub>2</sub>]<sub>2</sub>," *Phys. Rev. B* **77**, 104413 (2008).
- <sup>11</sup> Oleksii I. Motrunich, "Variational study of triangular lattice spin-1/2 model with ring exchanges and spin liquid state in  $\kappa$ -(ET)<sub>2</sub>Cu<sub>2</sub>(CN)<sub>3</sub>," *Phys. Rev. B* **72**, 045105 (2005).
- <sup>12</sup> Sung-Sik Lee and Patrick A. Lee, "U(1) Gauge Theory of the Hubbard Model: Spin Liquid States and Possible Application to  $\kappa$ -(BEDT-TTF)<sub>2</sub>Cu<sub>2</sub>(CN)<sub>3</sub>," *Phys. Rev. Lett.* **95**, 036403 (2005).
- <sup>13</sup> William Witczak-Krempa, Gang Chen, Yong Baek Kim, and Leon Balents, "Correlated quantum phenomena in the strong spin-orbit regime," *Annual Review of Condensed Matter Physics* **5**, 57–82 (2014).
- <sup>14</sup> Gang Chen and Leon Balents, "Spin-orbit effects in Na<sub>4</sub>Ir<sub>3</sub>O<sub>8</sub>: A hyper-kagome lattice antiferromagnet," *Phys. Rev. B* **78**, 094403 (2008).
- <sup>15</sup> Gang Chen, Rodrigo Pereira, and Leon Balents, "Exotic phases induced by strong spin-orbit coupling in ordered double perovskites," *Phys. Rev. B* **82**, 174440 (2010).
- <sup>16</sup> Haruki Watanabe, Hoi Chun Po, Ashvin Vishwanath, and Michael Zaletel, "Filling constraints for spin-orbit coupled insulators in symmorphic and nonsymmorphic crystals," *Proceedings of the National Academy of Sciences* **112**, 14551–14556 (2015).
- <sup>17</sup> A. Olariu, P. Mendels, F. Bert, F. Duc, J. C. Trombe, M. A. de Vries, and A. Harrison, "<sup>17</sup>O NMR Study of the Intrinsic Magnetic Susceptibility and Spin Dynamics of the Quantum Kagome Antiferromagnet ZnCu<sub>3</sub>(OH)<sub>6</sub>Cl<sub>2</sub>," *Phys. Rev. Lett.* **100**, 087202 (2008).
- <sup>18</sup> Tian-Heng Han, Joel S Helton, Shaoyan Chu, Daniel G Nocera, Jose A Rodriguez-Rivera, Collin Broholm, and Young S Lee, "Fractionalized excitations in the spin-liquid state of a kagome-lattice antiferromagnet," *Nature* **492**, 406–410 (2012).
- <sup>19</sup> Mingxuan Fu, Takashi Imai, Tian-Heng Han, and Young S Lee, "Evidence for a gapped spin-liquid ground state in a

- kagome Heisenberg antiferromagnet,” *Science* **350**, 655–658 (2015).
- <sup>20</sup> Tian-Heng Han, MR Norman, J-J Wen, Jose A Rodriguez-Rivera, Joel S Helton, Collin Broholm, and Young S Lee, “Correlated impurities and intrinsic spin liquid physics in the kagome material Herbertsmithite,” arXiv preprint arXiv:1512.06807 (2015).
- <sup>21</sup> Daisuke Yamamoto, Giacomo Marmorini, and Ippai Danshita, “Quantum Phase Diagram of the Triangular-Lattice XXZ Model in a Magnetic Field,” *Phys. Rev. Lett.* **112**, 127203 (2014).
- <sup>22</sup> Daniel Sellmann, Xue-Feng Zhang, and Sebastian Eggert, “Phase diagram of the antiferromagnetic XXZ model on the triangular lattice,” *Phys. Rev. B* **91**, 081104 (2015).
- <sup>23</sup> Changle Liu, Xiaoqun Wang, and Rong Yu, “Semiclassical ground-state phase diagram and multi-q phase of a spin-orbit coupled model on triangular lattice,” arXiv preprint 1607.02295 (2016).
- <sup>24</sup> Doron Bergman, Jason Alicea, Emanuel Gull, Simon Trebst, and Leon Balents, “Order-by-disorder and spiral spin-liquid in frustrated diamond-lattice antiferromagnets,” *Nature Physics* **3**, 487–491 (2007).